2104181 Pitfalls of seismic interpretation in prestack time- vs. depth-migration data

Tengfei Lin[1], Hang Deng[1], Zhifa Zhan[2], Zhonghong Wan[2], Kurt Marfurt[1]

1. School of Geology and Geophysics, University of Oklahoma, Norman, OK, United States.

2. BGP Inc., CNPC, Zhuozhou, Hebei, China.

Summary

In general depth migration is necessary in the presence of strong lateral velocity variation and avoids some of pitfalls that occur in time migrated data (Table 1). First, fault shadows can give rise to a 2nd (artificial) discontinuity coherence images computed from time migrated data. Such artifacts are removed in accurate velocity depth migrated data. Second, velocity pull-up and push down caused by the lateral changes in the overburden such as carbonate buildups and incised valleys will give rise to erroneous curvature anomalies in time-migrated data. These artifacts disappear in in properly depth-migrated data. Third, in complex structure time migrated data may be poorly focused. Fault termination of reflectors may be misaligned, giving rise to "wormy" coherence anomalies. Channel and other stratigraphic features may be diffuse (as reported by Rietveld et al., 1999) making them hard to interpret.

Attributes on time migrated data	Attributes on depth migrated data
Coherence sees fault shadows as a 2nd discontinuity	Fault shadows are removed, coherence sees the fault
Curvature sees velocity pull-up and push-down as structural artifacts	Velocity pull-up and push-down are removed; curvature sees true structure
Spectral components tune at a given time thickness	Spectral components tune at the true depth thickness

Table 1. Attribute comparison of time- vs. depth-migrated data.

Introduction

Coherence algorithm measure lateral changes in seismic waveform. (Bahorich and Farmer, 1995, 1996). Like other attributes, coherence is sensitive to noise. To avoid this problem, Kirlin (1992), Marfurt et al. (1998), and Gersztenkorn and Marfurt (1996a, 1996b, 1999) introduced more robust multitrace semblance- and eigenstructure-based coherence algorithms which provided improved images in the presence of random noise.

In contrast to random noise, all coherence algorithms are sensitive to fault shadows seen in time-migrated data. Fagin (1991) uses forward ray trace modeling to illustrate the fault shadow problem. A more complete description of the "fault whisper" problem on prestack data is given by Hatchell (2000). Fault whisper is the phenomenon of transmission distortions, which are produced by velocity changes across buried faults and unconformities and related to the phenomenon known as fault shadows.

Depth migrated data presents its own challenges. In time-migration the major impact of velocity is to focus or defocus reflectors and diffractors with some lateral movement. In depth-migration, these features are also moved both laterally and vertically. If the velocity model is inaccurate, depth migration may be inferior to time migrated data. Even if the data are properly imaged, the wavelet spectrum is no longer in Hertz, but in wavenumber which decreases with increasing velocity of deeper data.

Methodology

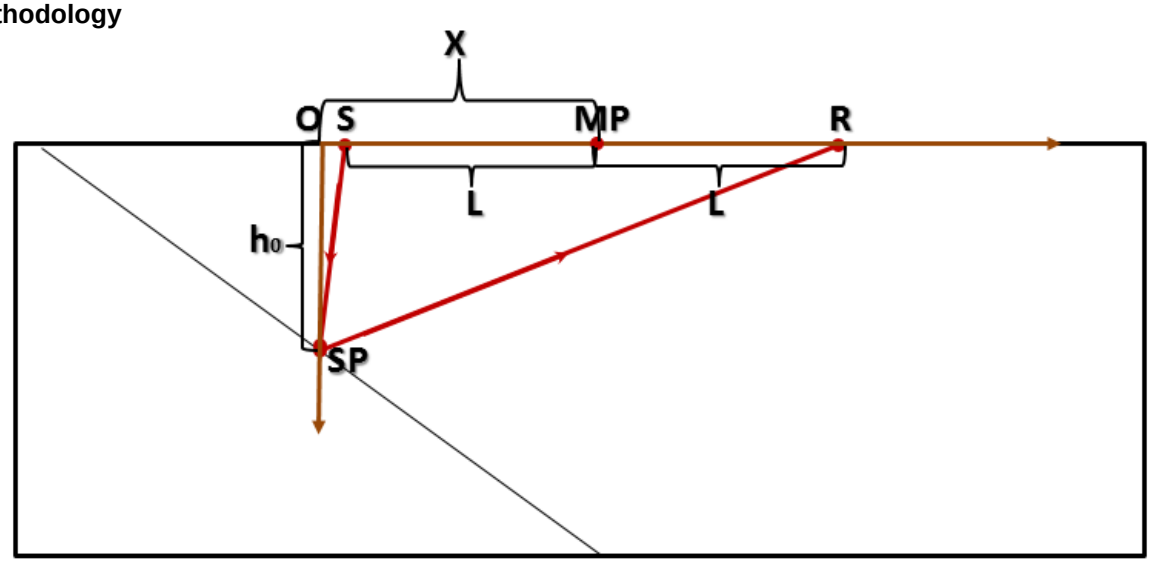

Figure 1. The geometry of PSTM. S: Source, R: Receiver, MP: Midpoint of the source and receiver, SP: Scatter point of sub-surface; X: the distance between point O and MP, L: the distance source and midpoint as well as midpoint and receiver. h0: the depth of the scatter point.

For the Kirchhoff prestack migration (PSTM), the total traveltime t is the sum of source to scatter point time t_s and the scatter point to receiver time t_r:

$$t = t_s + t_r \ , \qquad (1)$$

Assuming that the velocity V is constant, equation 1 can be expanded to:

$$t = \left[\frac{h_0^2+(x+l)^2}{V^2}\right]^{1/2} + \left[\frac{h_0^2+(x-l)^2}{V^2}\right]^{1/2} , \qquad (2)$$

where h_0 is the depth of the scatter point, x is the location of the source-receiver midpoint (MP), h is half the source-receiver offset.

Considering that:

$$t_0 = \frac{2h_0}{V_{avg}} , \qquad (3)$$

where V_{avg} is the average velocity for the two-way zero-offset time.

Therefore, equation 2 can be modified to:

$$t = \left[\left(\frac{t_0}{2}\right)^2 + \frac{(x+l)^2}{V_{rms}^2}\right]^{1/2} + \left[\left(\frac{t_0}{2}\right)^2 + \frac{(x+l)^2}{V_{rms}^2}\right]^{1/2} , \ (4)$$

where V_{rms} is the migration velocity, which is approximate to the RMS velocity for the horizontal cake model.

Figure 2 indicates us a fault model as well as its PSTM seismic profile. The purple and green horizons indicate us two high velocity zone.

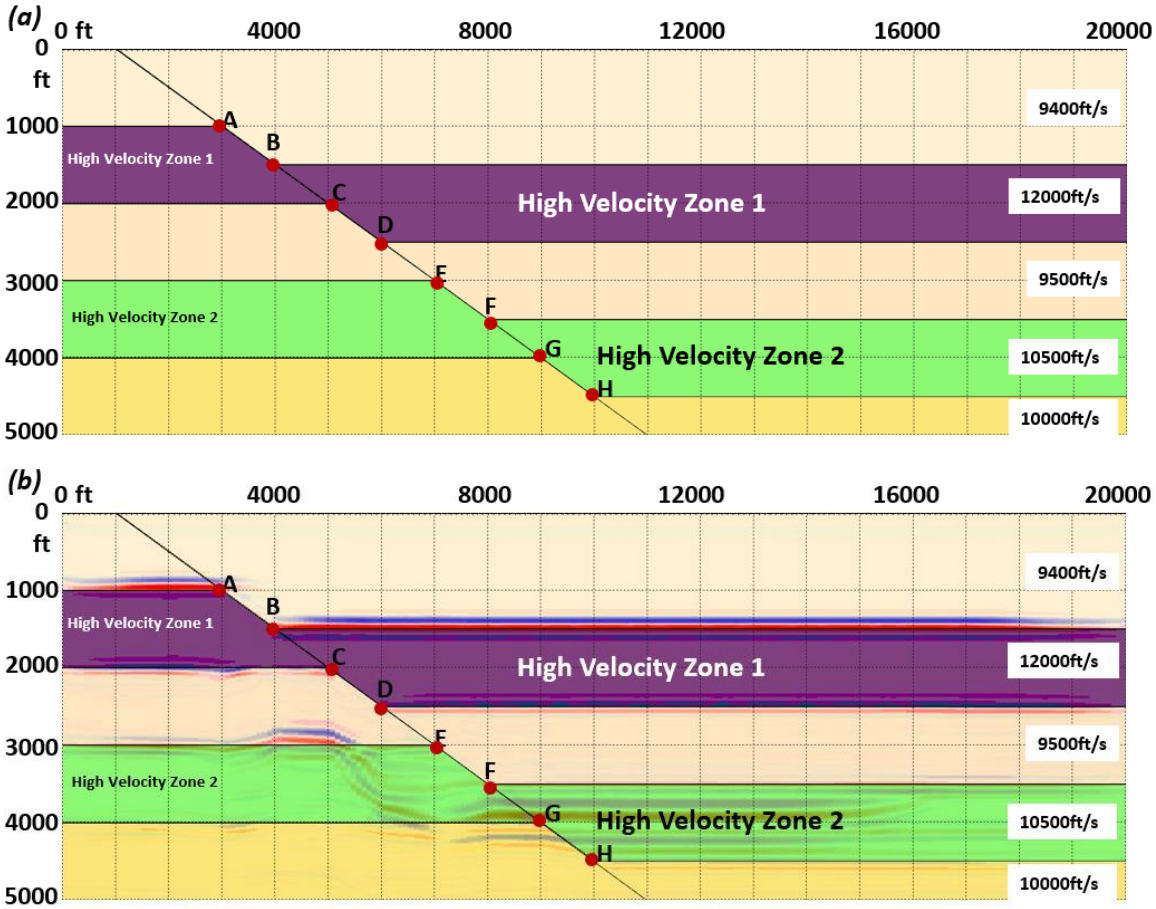

Figure 2. (a) The fault model; (b) the PSTM seismic profile of (a).

Pitfall

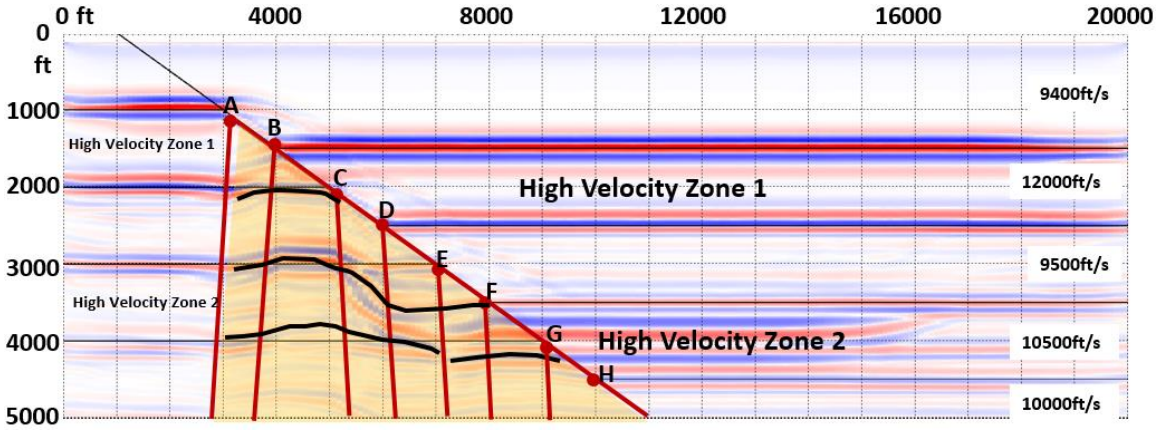

Figure 3. The PSTM seismic profile of the fault model.

Looking in detail at these oscillations in Figrue 3, point A-H are the points located at the main fault of the model. The semi-transparent yellow zone indicates the fault shadow zone, which is seriously disordered compared to the original structural model. Zone 1 push-down is marked between point A and

B, zone one pull-up is marked between point B and D. While Zong 2 push-down is marked between point F and G. On the time section a near-vertical structural axis can be drawn which links the position of each of these anomalies for each underlying reflection. These axes are a predictable consequence of extensional faulting of the sequence of velocity units that occur in this study area. In the real data example presented later they are shown to occur in each fault block (Fagin, 1991). Both the push-down and pull-up phenomenon are the time anomalies, which can be explained using zero-offset two-way travel time. The former one will generate trough, because of the slower traveltime; while the second type will generate crest because of the faster traveltime.

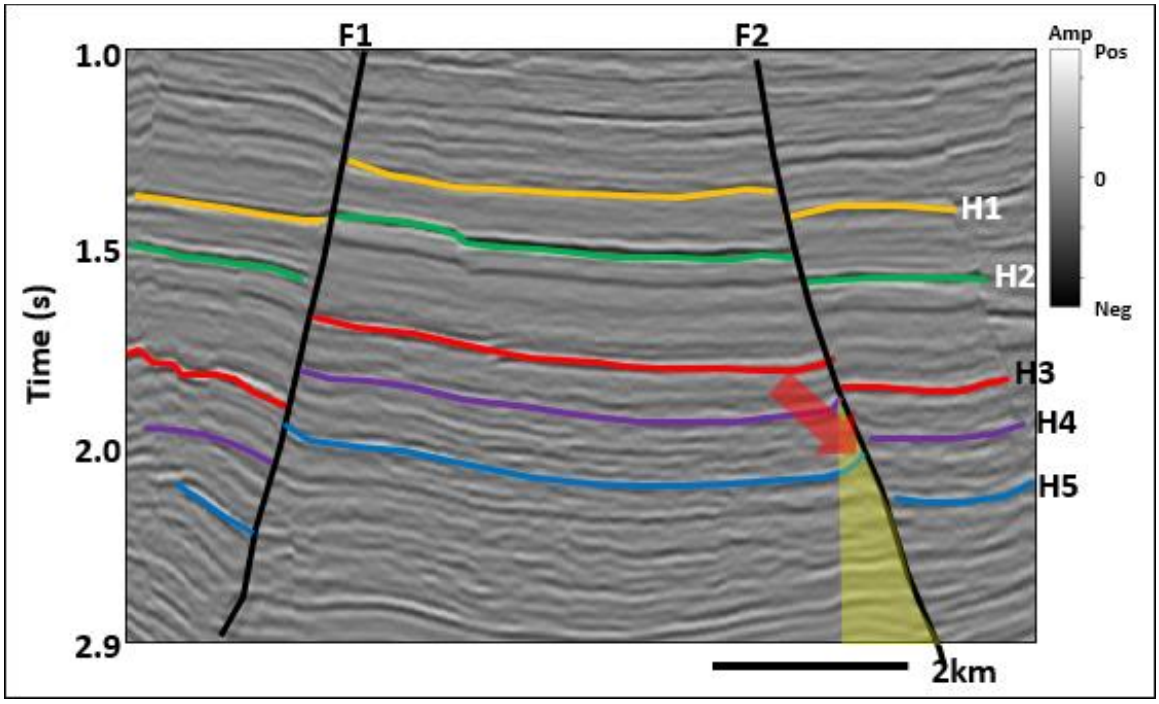

Figure 4. Seismic profile of PSTM amplitude volumes.

Figure 4 indicate us the seismic profile of PSTM amplitude volumes. The survey is located in Huabei Province, which was acquired by BGP Inc, China Natiional Petroleum Coporation.

F1 and F2 are two major faults and H1-H5 are horizons in the seismic profile. Seismic pitfalls (pull-up) are indicated by red arrows, which should be caused by the existence of high velocity zone between H3 and H5. The structural high zone seems unreasonable. This is because they are at upthrow, which means they should be structural low zone.

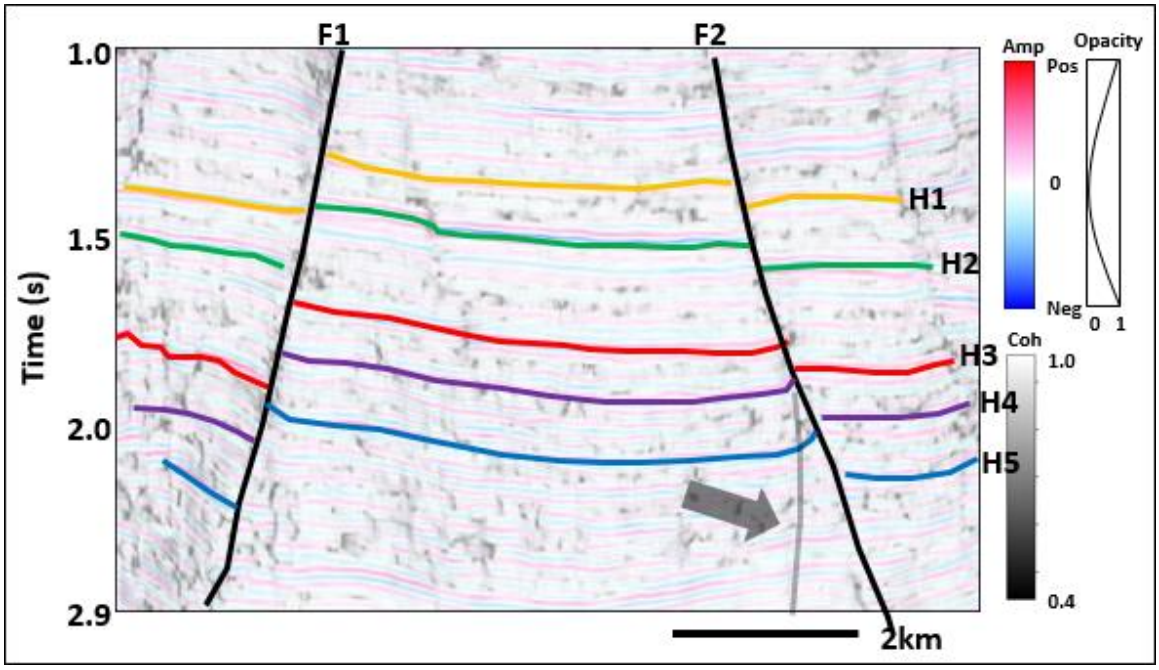

Figure 5. Vertical slice though coherence co-rendered with seismic amplitude for PSTM data.

Coherence is an important aid in fault interpretation. Figure 5 indicates the vertical slice though coherence co-rendered with seismic amplitude for PSTM data. The grey curved solid line indicated by grey arrow ban be interpreted as sub-fault splays to the main fault F2.

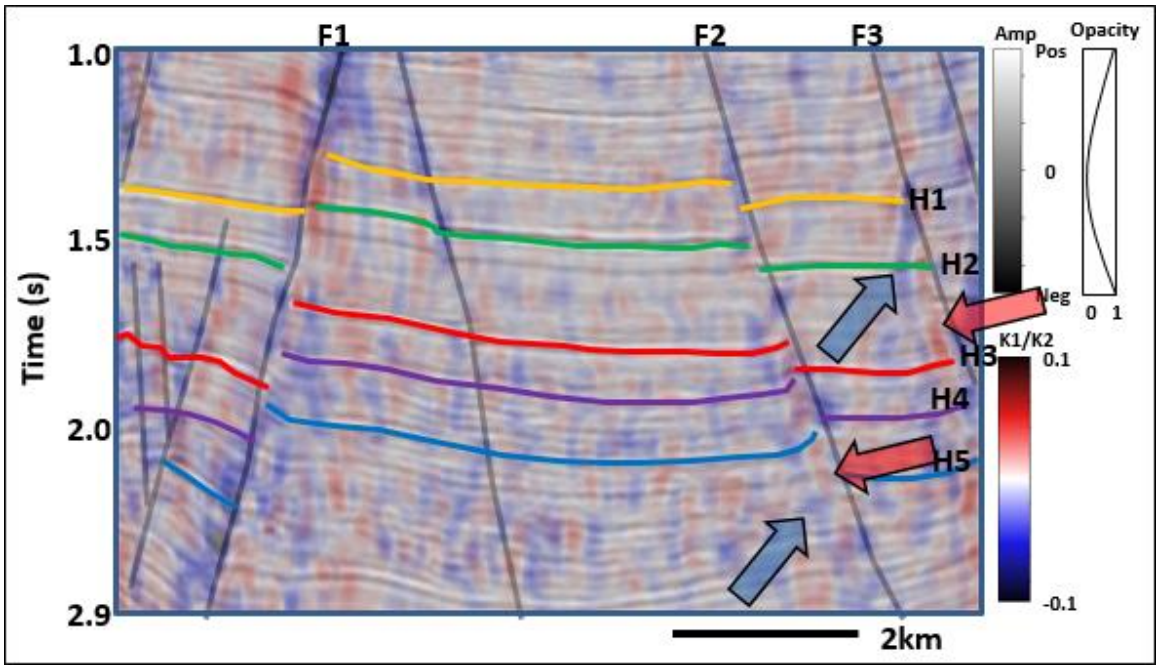

Figure 6. Vertical slice though most positive curvature co-rendered with most negative curvature (with long wavelet) and seismic amplitude along for PSTM data.

I co-render the most-positive curvature, most-negative curvature and seismic amplitude of time migrated and depth migrated data in Figure 6. The blue zone indicated by blue arrows for fault F2 and F3

indicates the syncline with most negative curvature, while the red zone indicated by red arrows for fault F2 and F3 indicates the anticline with most positive curvature.

Considering that F2 and F3 are normal faults, the parallel most positive- and negative- curvature seems unreasonable.

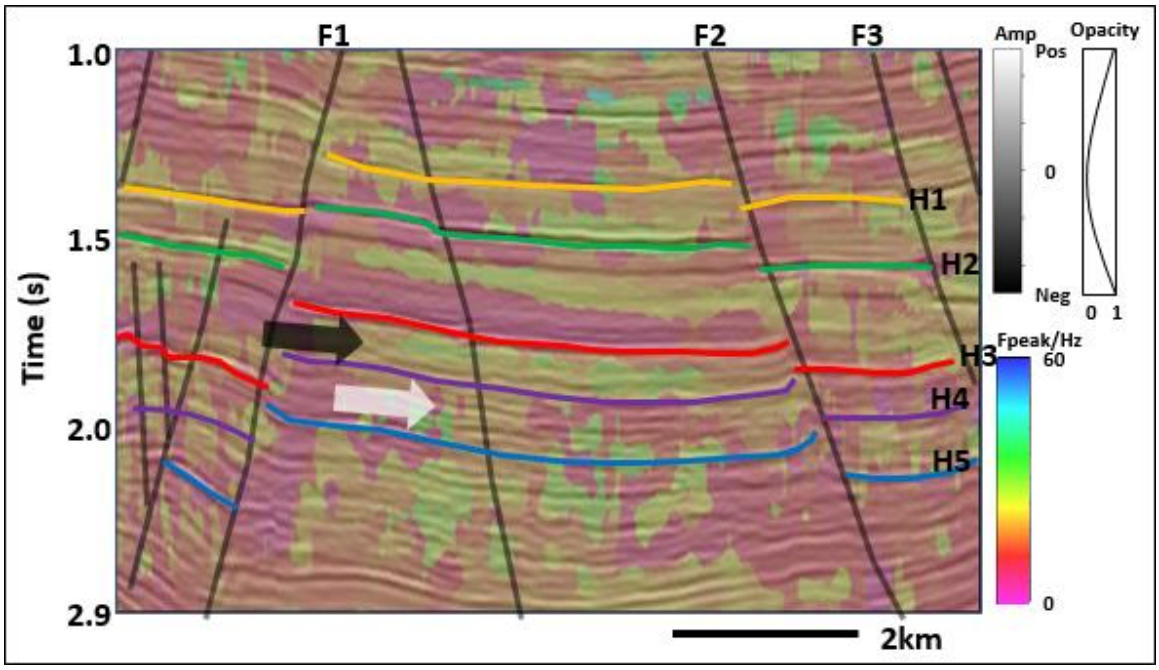

Figure 7. Vertical slice though peak frequency co-rendered with seismic amplitude for PSTM data.

Figure 7 indicates the vertical slice though peak frequency co-rendered with seismic amplitude for PSTM data. The black arrow indicates the zone between horizon H3 and H4, which the peak frequency is about 30 Hz. While the white arrow indicates the zone between horizon H4 and H5, which the peak frequency is about 20Hz. The black arrow indicates a high velocity zone between horizon H3 and H4, which means it will be wider in depth than in time domain.

Mitigation

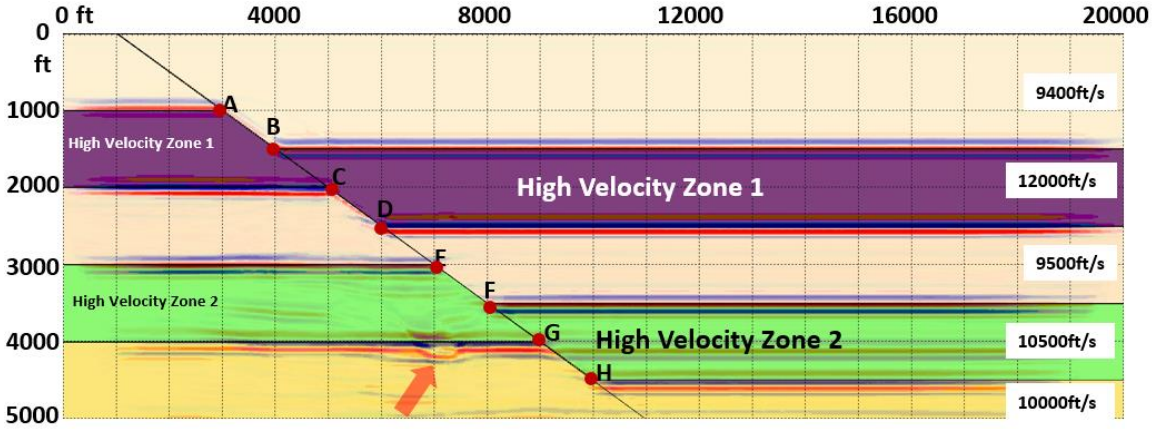

Figure 8. The PSTM seismic profile of the fault model.

Considering the pitfalls existed in seismic profile of the fault modal for PSTM in Figure 2 and 3. Figure 8 indicates that the seismic profile perfectly match the fault model except for the tiny zone pointed by red

arrow. The pitfalls (pull-up and push-down) in Figure 3 are removed in figure 8, compared to the prestack Kirchhoff depth migration seismic (PSDM) data.

Figure 8 indicates the seismic profile of PSTM amplitude volumes, which can accurately describe the structure compared to the figure 4. The pull-up zone indicated by red arrow as well as the fault shadow zone in figure 4 disappear in figure 9. The fault shadow zone can be described as the sub-fault splays to the main fault F2 in figure 5. Figure 10 indicates the vertical slice though coherence co-rendered with seismic amplitude for PSTM data, in which the sub-fault splays are removed. Figure 11 indicates vertical slice though most positive curvature co-rendered with most negative curvature (with long wavelet) and seismic amplitude along for PSTM. The parallel syncline and anticline indicated by blue and red arrows in figure 6 disappear in figure 11, which correct lots of structural pitfalls.

Figure 12 indicates the vertical slice though peak frequency co-rendered with seismic amplitude for PSTM data. We can found that the peak frequency in time domain is about twice for the peak wavenumber in depth domain. The black and white arrow in figure 12 indicate the relevant zones in figure 7. The peak wavenumber is 13 cycles/wavenumber for the zone targeted by both black and white zone, which shows the different situation in time domain in figure 7. This is because the existence of the high velocity zone indicated by black arrow, which extends the horizons.

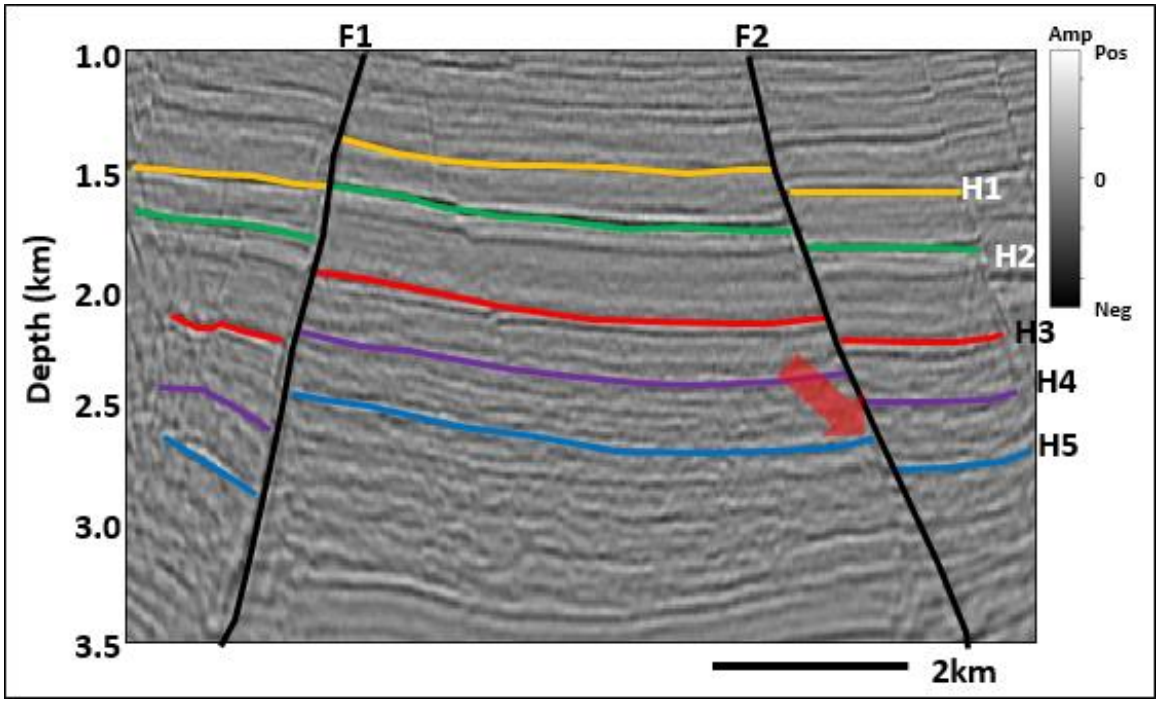

Figure 9. Seismic profile of PSDM amplitude volumes.

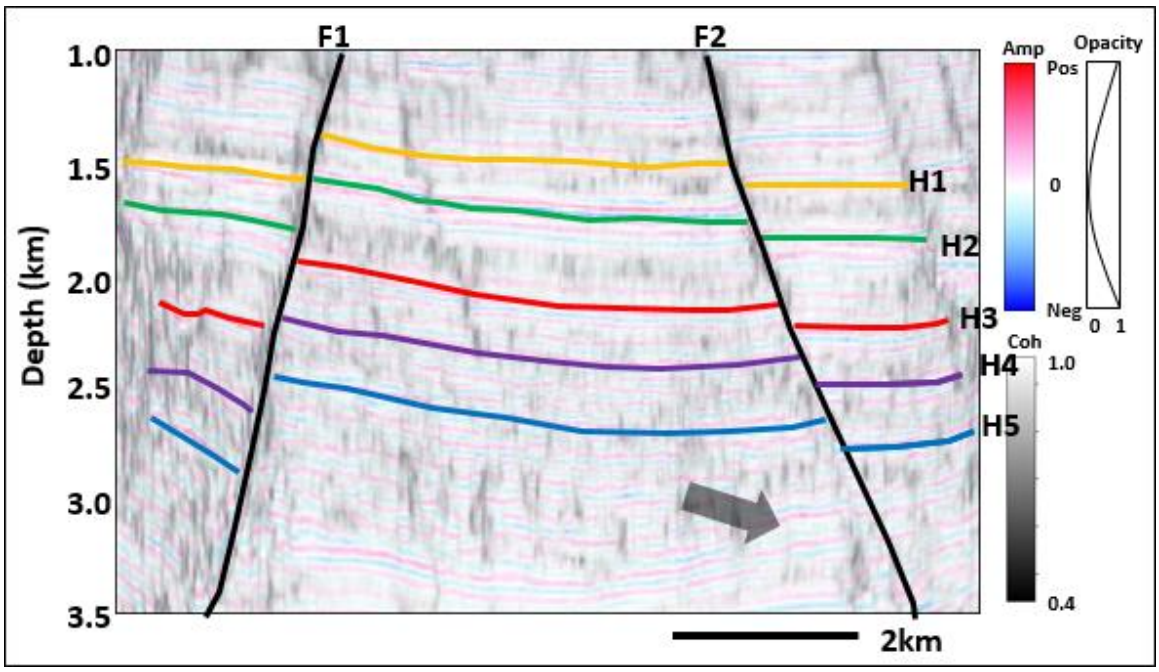

Figure 10. Vertical slice though coherence co-rendered with seismic amplitude for PSDM data.

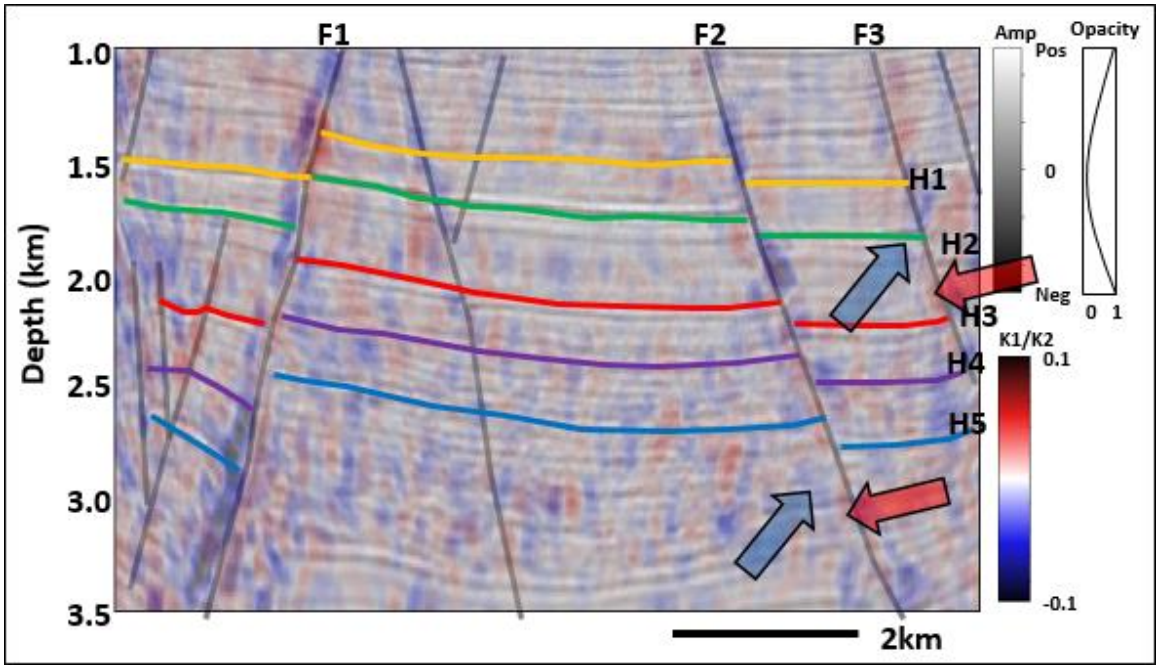

Figure 11. Vertical slice though most positive curvature co-rendered with most negative curvature (with long wavelet) and seismic amplitude along for PSDM data.

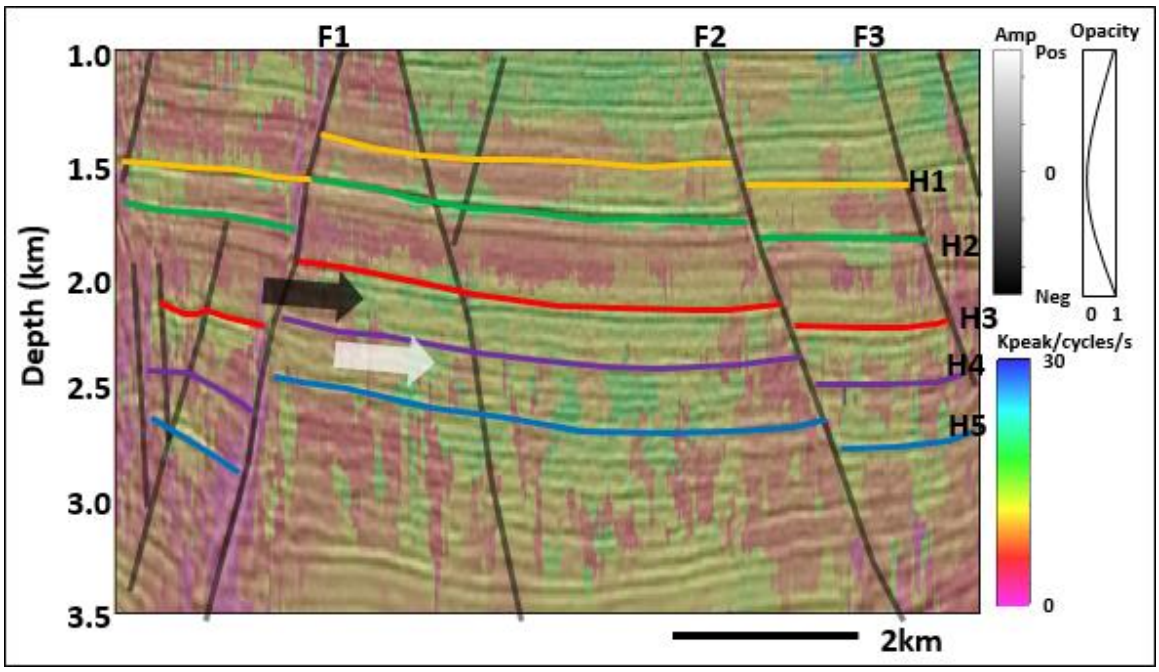

Figure 12. Vertical slice though peak frequency co-rendered with seismic amplitude for PSDM data.

Reference

Bahorich, M. S., and Farmer, S. L., 1995, 3-D seismic discontinuity for faults and stratigraphic features: The Leading Edge, 14, 1053–1058.

Bahorich, M. S., and Farmer, S. L., 1996, Methods of seismic signal processing and exploration: U.S. Patent 5 563 949.

Fagin, S.W., 1991, Seismic modeling of geologic structures: Applications to exploration problems: Geophysical dEvelopment series, 2. Society of Exploration Geophysics.

Gersztenkorm, A., and K. J. Marfurt, 1996, Eigenstructure based coherence computations, 66th Annual International Meeting, SEG, Expanded Abstracts, 328-331.

Gersztenkorm, A., and K. J. Marfurt, 1999, Eigensturcture based coherence computations as an aid to 3-D structural and stratigraphic mapping: Geophysics, 64, 1468-1479.

Hatchell P. J., 2000, Fault whispers: Transmission distortions on prestack seismic reflection data: Geophysics, 65, 377 – 389.

Kirlin, R., 1992, The relationship between semblance and eigenstructure velocity estimators: Geophysics, 57, 1027-1033.

Marfurt, K. J., R. L. Kirlin, S. H. Farmer, and M. S. Bahorich, 1998, 3-D seismic attributes using a running window semblance-based coherency algorithm: Geophysics, 63, 1150-1165.

Rietveld, W. E., J. H. Kommedal, and K. J. Marfurt, 1999, The effect of prestack depth migration on 3D seismic attributes: Geophysics, 64, 1553-1561.